

Third-order depositional sequences reflecting Milankovitch cyclicity

André Strasser^{1*}, Heiko Hillgärtner¹, Wolfgang Hug¹ and Bernard Pittet²

¹*Institut de Géologie, Université de Fribourg, Pérolles, CH-1700 Fribourg, Switzerland;* ²*Centre Sciences de la Terre, Université de Lyon I, 27-43 bd. du 11 novembre 1918, F-69622 Villeurbanne cedex, France*

ABSTRACT

The origin of third-order depositional sequences remains debatable, and in many cases it is not clear whether they were controlled by tectonic activity and/or by eustatic sea-level changes. In Oxfordian and Berriasian–Valanginian carbonate-dominated sections of Switzerland, France, Germany and Spain, high-resolution sequence-stratigraphic and cyclostratigraphic analyses show that the sedimentary record reflects Milankovitch cyclicity. Orbitally induced insolation changes translated into sea-level fluctuations, which in turn controlled accommodation changes. Beds and bedsets formed in rhythm with the precession and 100-kyr eccentricity cycles, whereas the 400-kyr

eccentricity cycle contributed to the creation of major depositional sequences. Biostratigraphical data allow the correlation of many of the 400-kyr sequence boundaries with third-order sequence boundaries recognized in European basins. This implies that climatically controlled sea-level changes contributed to the formation of third-order sequences. Furthermore, this cyclostratigraphical approach improves the relative dating of stratigraphic intervals.

Introduction

There is considerable controversy about origin and duration of third-order depositional sequences (e.g. Miall, 1997). Depositional sequences are defined as stratigraphic units composed of a ‘relatively conformable succession of genetically related strata’ (Mitchum *et al.*, 1977) and result from accommodation changes that control production and distribution of the sediments building up these strata. Based on seismic stratigraphy, Vail *et al.* (1977) defined first-, second-, and third-order sequences with durations of 200–300 Myr, 10–80 Myr, and 1–10 Myr, respectively. When sequence stratigraphy began to be applied also to outcrops, time resolution increased. Thus, Vail *et al.* (1991) identified six orders of depositional sequences, lasting from tens of millions of years (first- and second-order) to a few 10-thousand years (sixth-order). The third-order sequences were said to have durations of 0.5–3 Myr (Haq *et al.*, 1987). The sequence-chronostratigraphic charts of Hardenbol *et al.* (1998) show numerous sequences with durations of 0.5 Myr or less (simply called ‘sequences’ on the charts but commonly referred to as ‘third-order

sequences’ in the various publications in the corresponding book edited by De Graciansky *et al.*, 1998).

First- and second-order sequences are related to tectonic and tectono-eustatic changes, whereas fourth-, fifth- and sixth-order sequences are explained by climatically controlled sea-level fluctuations in the Milankovitch frequency band (e.g. Vail *et al.*, 1991; Plint *et al.*, 1992; Read, 1995). Third-order sequences are often seen as resulting from a combination of tectonic and glacio-eustatic accommodation changes (Vail *et al.*, 1991). However, Cloetingh (1988) argued that such sequences can also form uniquely through changes in intraplate stress, and Dewey and Pitman (1998) doubt that global eustasy can overrule local and regional tectonics. Miall (1990) suggested that third-order cyclicity may result from a combination of plate rifting and convergence superimposed on second-order volume changes of mid-ocean ridges.

Based on detailed outcrop studies, high-resolution sequence-stratigraphic and cyclostratigraphic analyses were performed in carbonate-dominated sediments of the Oxfordian in Switzerland, Germany, and Spain, and of the Berriasian–Valanginian in Switzerland and France. These sediments were deposited in a passive-margin setting along the northern border of the Tethys ocean (Dercourt *et al.*, 1993). Differential subsidence created

locally varying sediment thicknesses but did not cause long-lasting gaps (Pittet, 1996; Hillgärtner, 1998, 1999; Hug, 2001). Our interpretations suggest that, at least for the studied intervals, the formation of the ‘third-order sequences’ identified and dated by Hardenbol *et al.* (1998) in European basins is closely related to the 400-kyr eccentricity cycle of the Earth’s orbit.

High-resolution sequence stratigraphy and cyclostratigraphy

Measurements were made of 22 Middle to Upper Oxfordian sections and 17 Berriasian to Lower Valanginian sections (Strasser, 1994; Pasquier and Strasser, 1997; Pittet and Strasser, 1998a,b; Hillgärtner, 1999; Hug, 2001). Microfacies analysis was carried out on some 3500 samples. Most sections represent shallow carbonate-dominated platform environments, but deeper-water sections were also logged to permit platform-to-basin correlations. For the purpose of this paper, two sections from the Oxfordian and two from the Berriasian–Valanginian (Fig. 1) are presented.

All studied sections display distinct hierarchical stacking patterns and facies evolutions, which allow the identification of depositional sequences (or sedimentary cycles) at different scales (example shown in Fig. 2). The smallest unit where facies evolution implies one cycle of environmental

*Correspondence: André Strasser, Institut de Géologie, Université de Fribourg, Pérolles, CH-1700 Fribourg, Switzerland. E-mail: andreas.strasser@unifr.ch



Fig. 1 Location of the four stratigraphic sections presented in this paper.

change (including sea-level change) is called an elementary sequence. These group into small-scale sequences, which in turn form medium-scale sequences; these then build up large-scale sequences (for definitions see Strasser *et al.*, 1999).

In platform sections, on each hierarchical level, facies evolution generally indicates deepening and shallowing trends. As a consequence of superposition of high-frequency sea-level fluctuations on a longer-term trend of sea-level change, surfaces of elementary or small-scale sequences indicating lowest accommodation (including emersion and erosion) commonly are repeated and define a sequence-boundary zone (Montañez and Osleger, 1993; Figs 2–4). Maximum-flooding surfaces are not always developed, but the (relatively) deepest facies indicate an interval corresponding to the fastest creation of accommodation space. It is common that 2–6 elementary sequences stack into a small-scale sequence, and that 4 small-scale sequences build up a medium-scale one. Bed-by-bed correlations between the sections show that, on the shallow platform, elementary or small-scale sequences can be missing if

low accommodation did not permit their deposition or caused erosion (e.g. Salève section, Fig. 4). Chronostratigraphic tie points in the platform sections are provided by benthic foraminifera calibrated with ammonite zones in the Berriasian (Clavel *et al.*, 1986), and by some rare ammonites and mineralo-stratigraphic correlations in the Oxfordian (Gygi and Persoz, 1986; Gygi, 1995).

In the deeper-water sections of the Swabian Jura (Oxfordian), many carbonate beds contain sponges (Fig. 3). The micritic matrix stems mainly from carbonate mud exported from the adjacent shallow carbonate platform (preferentially during transgression when carbonate productivity is high on the platform, and during sea-level fall forcing progradation of the platform; Schlager *et al.*, 1994; Pittet and Strasser, 1998a). Marly layers correspond to flooding of the platform or to emersion when only a small amount of carbonate mud is exported to the basin. Furthermore, carbonate productivity and input of clay minerals were also modulated by climate changes. Elementary sequences correspond to one or two limestone–marl alternations, depending on the availability of carbonate mud (Pittet and Strasser, 1998a). Small-scale sequences commonly display nodular horizons resulting from increased bioturbation, which is interpreted as corresponding to condensation during rapid sea-level rise. Sequence boundaries of small- and medium-scale sequences are inferred at the base of relatively thick carbonate beds, but it is easier to define these sequences by their condensed sections (Fig. 3). Large-scale sequence boundaries are placed at the base of intervals with relatively thick carbonate beds (no sequence boundary is inferred at the base of the sponge bioherm in small-scale sequence 4' because it is local and grades laterally into marls). The sections of the Swabian Jura are well dated by ammonites (Schweigert, 1995; Schweigert and Callomon, 1997).

In the deep-water sections of the Vocontian Basin (Berriasian–Valanginian), thickening-up trends define bundles composed of 3–6 limestone–marl alternations (Fig. 4). One alternation corresponds to an elementary sequence on the platform (Pasquier and Strasser, 1997), and the bundles

can be compared to the small-scale sequences. Medium-scale sequences are not well developed in the basin and can be inferred only from platform-to-basin correlation. Large-scale sequence boundaries are placed at the base of relatively thick carbonate beds and/or slumps (Strohmenger and Strasser, 1993). The sections are dated by ammonites and calpionellids (Le Hegarat, 1971).

The correlations shown in Figs 3 and 4 are based on biostratigraphical and sequence-stratigraphic criteria and represent best-fit solutions, also integrating other sections (Pittet and Strasser, 1998a,b; Hillgärtner, 1999; Hug, 2001). The relatively good biostratigraphical control allows the correlation of the identified medium- or large-scale sequence boundaries (or sequence-boundary zones) with the sequence boundaries of Hardenbol *et al.* (1998). Based on the absolute dating by Gradstein *et al.* (1995), Hardenbol *et al.* attributed ages to biozone boundaries as well as to sequence boundaries (Fig. 5). Despite the error margins of absolute dating, a relative time framework thus is given, which allows the duration of the elementary, small-scale, and medium-scale sequences to be estimated (Fig. 6).

In the Oxfordian platform section of Court, between 52 and 59 elementary sequences are counted between sequence boundaries Ox6 and Ox8, depending on the exclusion or inclusion of sequence-boundary zones (Fig. 3; see also Fig. 2 for definition of elementary sequences). Considering that Hardenbol *et al.* (1998) attribute 1.2 Myr to the interval between these two sequence boundaries, it is implied that one elementary sequence corresponds to 20–23 kyr. This is close to the duration of the orbital precession cycle with a period of about 20 kyr in Late Jurassic to Early Cretaceous times (Berger *et al.*, 1989). The same interval contains 10 (respectively 12) small-scale sequences, suggesting that these formed in tune with the first eccentricity cycle of 100 kyr. Four small-scale sequences build up a medium-scale one, which would correspond to the second eccentricity cycle of 400 kyr. In the deeper-water section of Balingen–Tieringen, the numbers of small- and medium-scale sequences found between Ox6 and Ox8 are comparable to

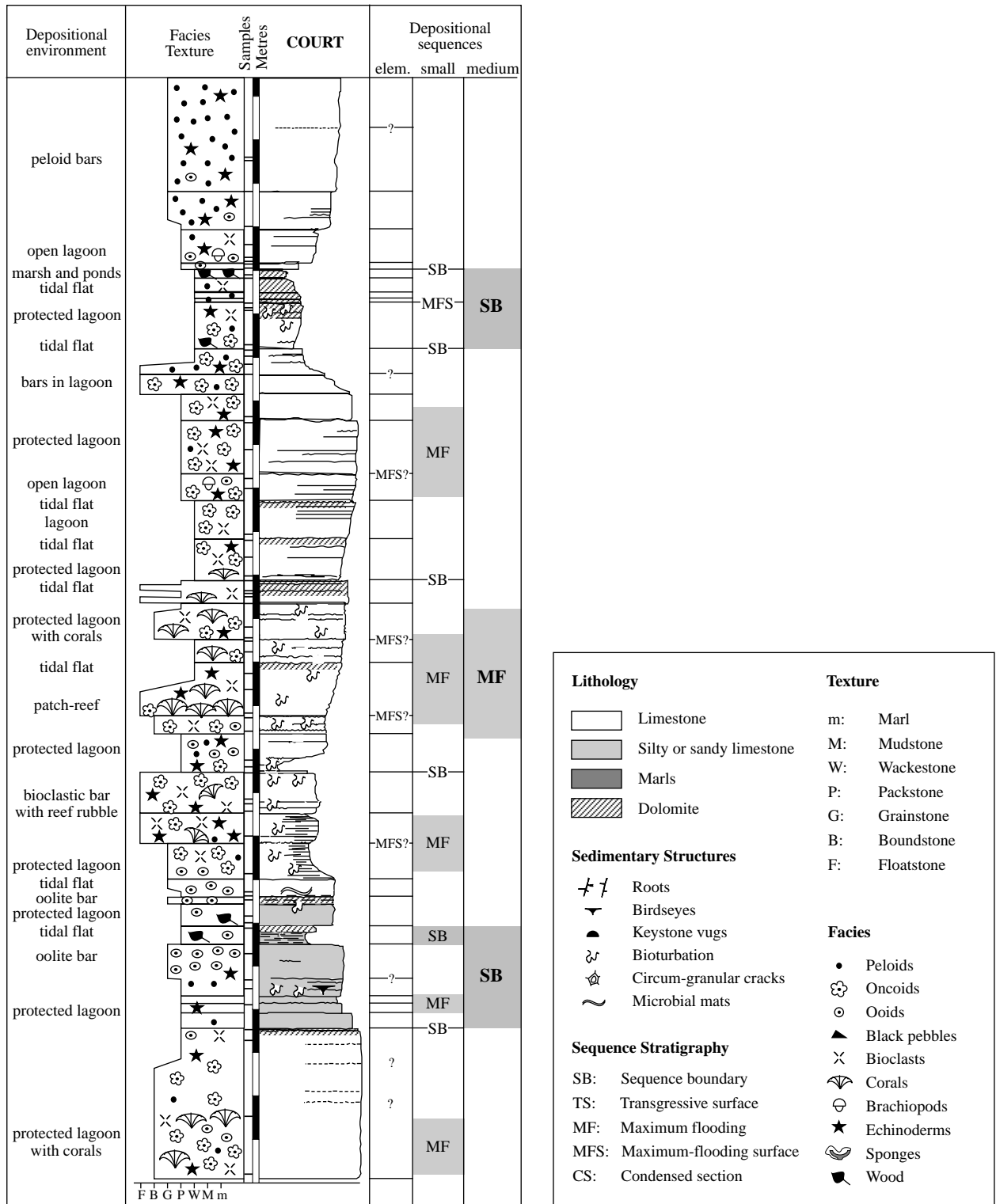


Fig. 2 Example of hierarchical stacking of elementary sequences into small- and medium-scale depositional sequences. When accommodation is low, elementary sequences generally correspond to one bed; higher accommodation may allow the development of a maximum-flooding surface. Sequence-boundary zones (grey) develop when several elementary or small-scale sequences form pronounced sequence boundaries. Maximum-flooding zones (grey) are indicated by relatively deepest facies. Upper Oxfordian of Court section, Switzerland (see also Fig. 3).

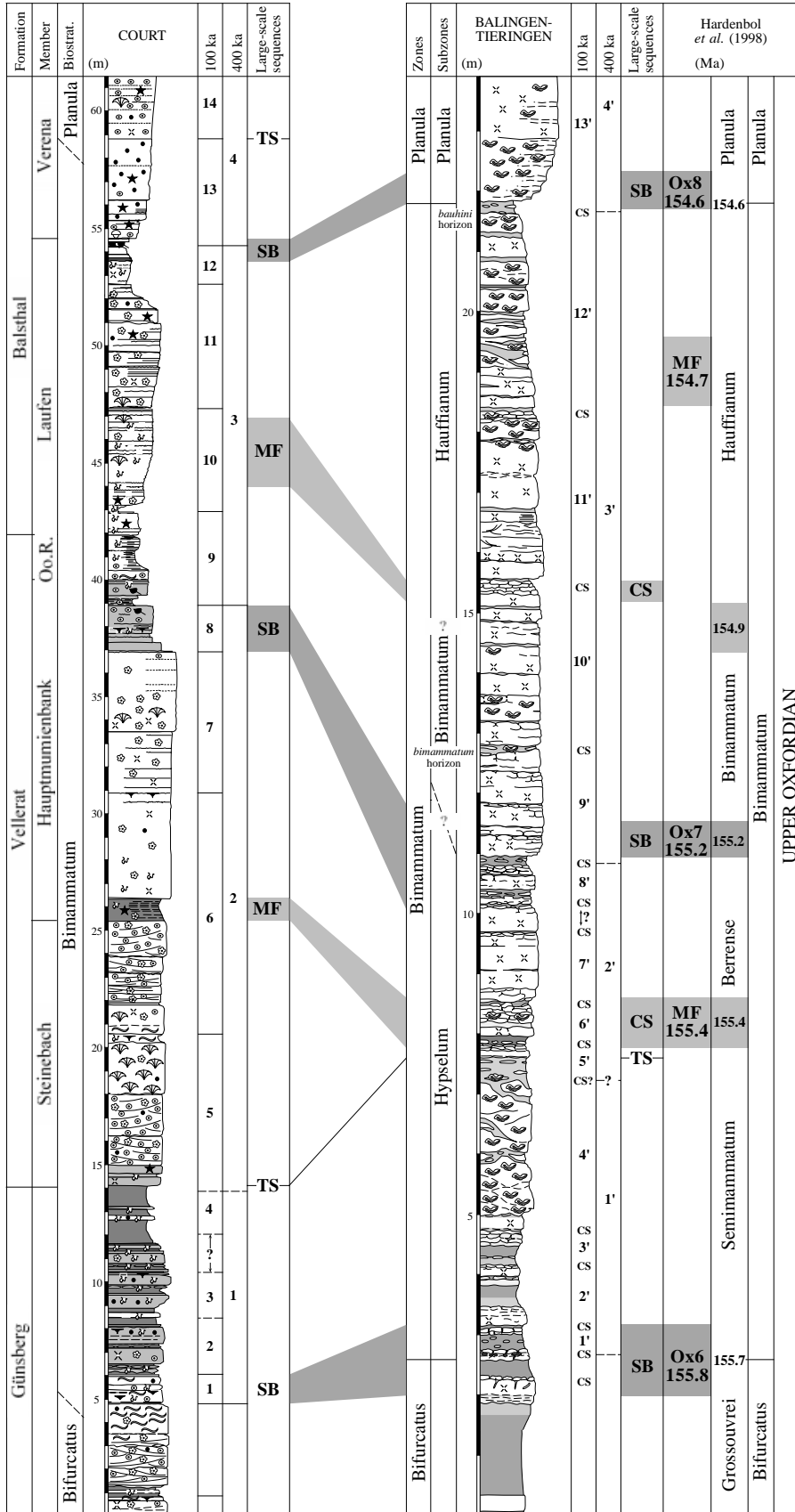


Fig. 3 Lithostratigraphy, biostratigraphy, sequence stratigraphy and cyclostratigraphy of the Upper Oxfordian in the Court and Balingen-Tieringen sections, and comparison with the chart of Hardenbol *et al.* (1998). Ammonite zones and subzones in Balingen-Tieringen according to Schweigert (1995), litho- and biostratigraphy in Court according to Gygi and Persoz (1986) and Gygi (1995). Distance between the two sections is 155 km. Note that the two sections have different scales. For legend see Fig. 2 (Oo.R., Oolithe rousse).

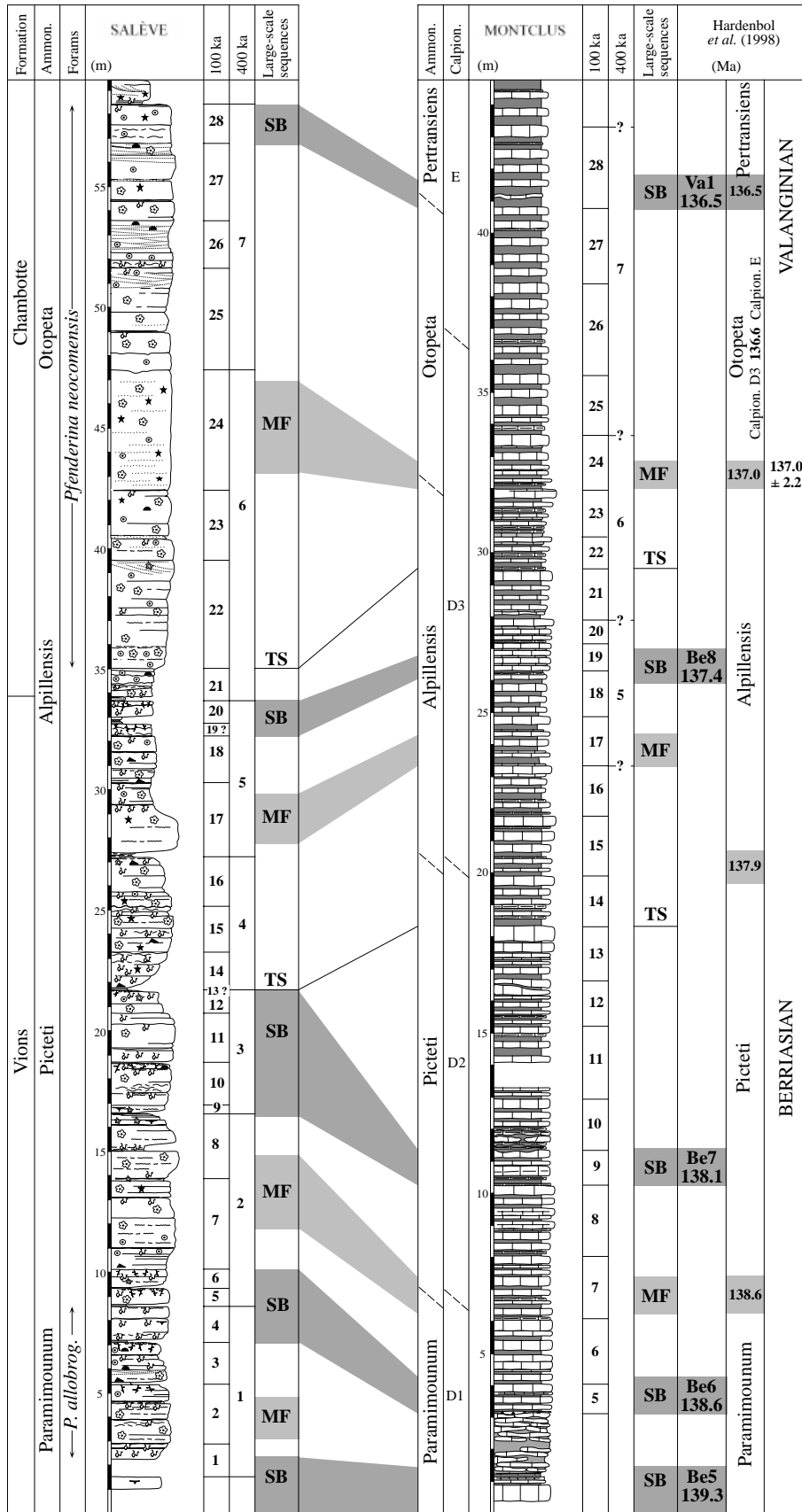


Fig. 4 Lithostratigraphy, biostratigraphy, sequence stratigraphy and cyclostratigraphy of the Upper Berriasian and Lower Valanginian in the Salève and Montclus sections, and comparison with the chart of Hardenbol et al. (1998). The benthic foraminifera *Pavlovecina allobrogensis* and *Pfenderina neocomensis* allow an approximate correlation with the ammonite zones (Clavel et al., 1986; Hillgärtner, 1999). Ammonite zonation in Montclus according to Le Hegarat (1971), calpionellid zones according to Hillgärtner (1999). Distance between the two sections is 190 km. Note that the two sections have different scales. For legend see Fig. 2.

	T-R facies cycles	Sequences	Ammonite		
			subzones	zones	
L. Valang.	regressive	136.49— SB Va 1 —MFS/CS—		Pertransiens 136.49	
				Otopeta	
Upper Berriasian	trans-gressive	137.44— SB Be 8 —MFS/CS—	136.99	Boissieri	
			Alpillensis		
		138.08— SB Be 7 —MFS/CS—	137.90		Picteti
	regressive	138.61— SB Be 6 —MFS/CS—	138.61		Paramimounum
		139.33— SB Be 5			

	T-R facies cycles	Sequences	Ammonite	
			subzones	zones
Upper Oxfordian	trans-gressive	154.63— SB Ox 8 —MFS/CS—	154.36	Planula
			Planula	
		154.89	Bimammatum	
	155.15— SB Ox 7 —MFS/CS—	Bimammatum		
	155.15	Berrense		
	regressive	155.81— SB Ox 6	155.42	Semimammatum
155.68			Grossouvrei	
155.94			Bifurcatus	
			Stenocycloides	

Fig. 5 Extracts from the chart of Hardenbol *et al.* (1998) to show biostratigraphical position and timing of the sequence boundaries (SB) and maximum-flooding surfaces (MFS) or condensed sections (CS) pertaining to this study, as well as the general transgressive–regressive trends.

those on the platform, although they are defined by condensed sections. Based on the dating by Hardenbol *et al.* (1998) and on the hierarchical stacking, it can be assumed that the formation of the observed depositional sequences was influenced by Milankovitch cycles.

Similar estimations can be made for the Berriasian–Valanginian interval (Fig. 4). Although some beds may be lost or repeated in slumps, and although elementary as well as some small-scale sequences may be strongly reduced or missing on the shallow platform, it is suggested that the elementary sequences correspond to the 20-kyr precession cycle, and the

small- and medium-scale sequences to the 100-kyr and 400-kyr eccentricity cycles, respectively (Fig. 6).

Discussion

As illustrated in the examples of Figs 3 and 4, many sequence-boundary zones of medium-scale sequences (attributed to the 400-kyr orbital eccentricity cycle) coincide, according to their biostratigraphical position, with sequence boundaries identified by Hardenbol *et al.* (1998). However, several discrepancies occur between the timing suggested by the cyclostratigraphical interpretation given herein and that indicated by Harden-

bol *et al.* In the Oxfordian example, the duration of the Bimammatum zone is 1.1 Myr according to Hardenbol *et al.* but 1.2 Myr according to the present interpretation, and the limits of the subzones are shifted by up to 200 kyr. Sequence boundary Ox7 is offset by 100–200 kyr, and MF154.7 of Hardenbol *et al.* occurs 100–200 kyr later than the large-scale condensed section (respectively maximum flooding) identified in the present study (Fig. 3). In the Berriasian–Valanginian sections, the timing of the biozones shows a fairly good correspondence (± 100 kyr), but discrepancies of up to 300 kyr occur between sequence boundaries (1.0 vs. 0.7 Myr between Be7 and Be8; 2.4 vs. 2.1 Myr between Be6 and Va1; see Fig. 4).

These discrepancies may be explained by local variations in basin morphology that shift the strongest lithological expression of a general sea-level fall or rise by one or several 100-kyr cycles, and/or by the difficulty in attributing ages with a resolution of 100 kyr to the biozones upon which the sequences are calibrated. Furthermore, during a long-term (second-order) trend of sea-level rise, maximum-flooding surfaces will be enhanced while sequence boundaries will be attenuated. During a long-term sea-level fall, the opposite will be true (Strasser *et al.*, 1999). If loss of accommodation related to the 400-kyr cycle was not important enough to create a clear facies contrast and/or diagnostic sedimentary structures, Hardenbol *et al.* (1998) did not attribute a ‘third-order’ sequence boundary.

On the shallow platform, the formation of depositional sequences of all scales is influenced directly by sea-level changes (autocyclically produced sequences can be identified by lateral correlation and are excluded from the cyclostratigraphical analysis). The fact that the hierarchical stacking of these sequences reflects the periodicities of Milankovitch cycles implies that the insolation changes received by the Earth must have translated into sea-level fluctuations. In the Late Jurassic and Early Cretaceous, ice in high latitudes and altitudes probably was present (Fairbridge, 1976; Frakes *et al.*, 1992; Eyles, 1993), but ice volumes were small and glacio-eustatic fluctuations were of low amplitude.

Oxfordian example (between SB Ox6 and SB Ox8)					
Sequence type	Number (including/excluding sequence boundary zones)		Inferred time span (ma)		Time span according to Hardenbol <i>et al.</i> (1998) (ma)
	Court	Balingen-Tieringen	Court	Balingen-Tieringen	
Elementary	59/52	difficult to define	1.18/1.04		155.8 - 154.6 = 1.2
Small-scale	12/10	13/11	1.2/1.0	1.3/1.1	
Medium-scale	3	3	1.2	1.2	

Berriasian-Valanginian example (between SB Bef6 and SB Va1)					
Sequence type	Number (including/excluding sequence boundary zones)		Inferred time span (ma)		Time span according to Hardenbol <i>et al.</i> (1998) (ma)
	Saleve	Montclus	Saleve	Montclus	
Elementary	difficult to define	110+/104+		2.2+/2.08+	138.6 - 136.5 = 2.1
Small-scale	24/20	24/22	2.4/2.2	2.4/2.2	
Medium-scale	6	difficult to define	2.4		

Fig. 6 Comparison of time between sequence boundaries as estimated by cyclostratigraphic analyses and as given by Hardenbol *et al.* (1998). It is inferred that elementary sequences correspond to the 20-kyr orbital precession cycle, and the small- and medium-scale sequences to the 100- and 400-kyr eccentricity cycles, respectively.

However, orbitally induced climate changes also caused thermal expansion and retraction of the uppermost layer of ocean water (Gornitz *et al.*, 1982), thermally induced volume changes in deep-water circulation (Schulz and Schäfer-Neth, 1998), and/or water retention and release in lakes and aquifers (Jacobs and Sahagian, 1993). These processes potentially contributed to low-amplitude sea-level changes (Plint *et al.*, 1992).

Berger *et al.* (1989) showed that the 100- and 400-kyr periodicities were relatively stable in the geological past, and that the precession cycle had a periodicity of about 20 kyr in the Late Jurassic to Early Cretaceous. The duration of the cycles implied by our study can thus be considered as a good approximation of the duration of hypothetical sea-level cycles, but amplitudes and shapes of the latter may have varied considerably.

The insolation curve published by Berger (1990) shows low-amplitude fluctuations around the 400-kyr cycle boundaries (Fig. 7). In the Jurassic–Cretaceous greenhouse world, low-amplitude insolation changes most probably caused low-amplitude sea-level changes (Read, 1995). Creation of accommodation space during the corresponding time interval generally was low, and sequence-boundary zones could potentially form. In the middle of a 400-kyr cycle, amplitudes of the 20- and 100-kyr pulses were higher, i.e. much accommodation was created in a short time but also rapidly lost. A possible result is illustrated in Fig. 2: just above the maximum flooding of a medium-scale (400-kyr) sequence allowing for the growth of coral reefs, a small-scale sequence boundary is underlined by important penecontemporaneous dolomitization.

Although these orbitally induced eustatic changes are global, their lithological expression depends strongly on regional and local factors. On shallow platforms, important sequence-boundary zones will form in tune with the 400-kyr cycle, but may be enhanced or attenuated according to the regional subsidence pattern or the long-term, tectono-eustatic trend of accommodation change. In deeper-water settings, lithologically well-marked sequence boundaries form mainly when sea-level falls related to Milankovitch cycles are enhanced by a long-term fall. Consequently, long-term accommodation changes created by tectonic and tectono-eustatic mechanisms define the general frame for the development of depositional sequences, but the orbital insolation cycles give the ‘beat’ for the making of beds and bedsets.

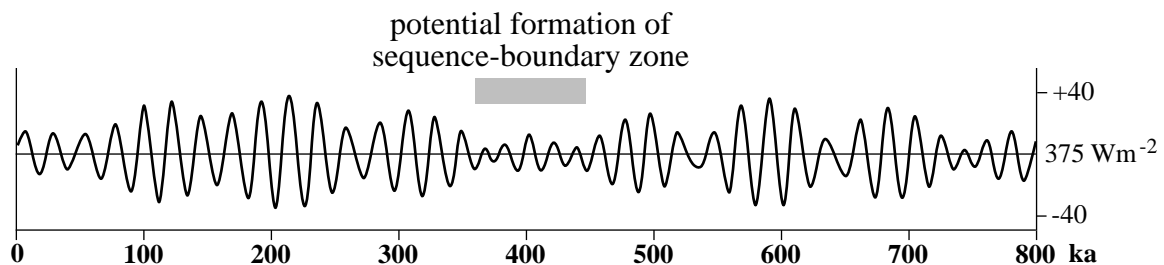


Fig. 7 Variations of September mid-month insolation at 30°N for the last 800 kyr (calculated by Berger, 1990). When low-amplitude insolation changes translate into low-amplitude sea-level fluctuations, a sequence-boundary zone may form. For discussion refer to text (Wm^{-2} = watts per square metre).

Conclusions

Detailed analysis of Upper Jurassic and Lower Cretaceous sections suggests that lithologically well-developed sequence boundaries formed in tune with the 400-kyr eccentricity cycle of the Earth's orbit. In many cases, these have been identified as third-order sequence boundaries and are used for basin-wide and basin-to-basin correlations (De Graciansky *et al.*, 1998). Their dating by Hardenbol *et al.* (1998) is based on the absolute time-scale of Gradstein *et al.* (1995), but the relatively large error margins do not allow to precisely estimate the duration of the depositional sequences and the associated biozones. The cyclostratigraphical approach potentially increases the precision of relative dating of stratigraphic intervals and thus opens the door for a better correlation of depositional sequences (e.g. D'Argenio *et al.*, 1999), and for quantification of sedimentary, diagenetic, and evolutionary processes. Astronomical timescales have already been established for the Plio-Pleistocene and Miocene (e.g. Lourens *et al.*, 1996; Lourens and Hilgen, 1997) and are combined with a sequence-stratigraphic interpretation (Pillans *et al.*, 1998). Calibrating the Oligocene–Miocene boundary by cyclostratigraphy, Shackleton *et al.* (2000) underlined the importance of the 400-kyr eccentricity cycle. The present study shows that cyclostratigraphy also can be used as a tool for improving time-resolution in older sedimentary successions.

Acknowledgements

We thank Elias Samankassou for critically reading a first version of the manuscript, and reviewers Bruno D'Argenio, Georges Gorin and Frits Hilgen for their helpful comments. The financial support by the Swiss National Science Foundation (grant no. 20-46625.96) is gratefully acknowledged.

References

- Berger, A., 1990. Paleo-insolation at the Plio–Pleistocene boundary. *Paléobiol. Continent.*, **17**, 1–24.
- Berger, A., Loutre, M.F. and Dehant, V., 1989. Astronomical frequencies for pre-Quaternary palaeoclimate studies. *Terra Nova*, **1**, 474–479.
- Clavel, B., Charollais, J., Busnardo, R. and Le Hegarat, G., 1986. Précisions stratigraphiques sur le Crétacé inférieur basal du Jura méridional. *Ecol. Geol. Helv.*, **79**, 319–341.
- Cloetingh, S., 1988. Intraplate stresses: a tectonic cause for third-order cycles in apparent sea level?. In: *Sea-Level Changes: an Integrated Approach* (C. K. Wilgus *et al.*, eds). *Spec. Publ. Soc. econ. Paleont. Miner. Tulsa*, **42**, 19–29.
- D'Argenio, B., Ferreri, V., Raspini, A., Amodio, S. and Buonocunto, F.P., 1999. Cyclostratigraphy of a carbonate platform as a tool for high-precision correlation. *Tectonophysics*, **315**, 357–385.
- De Graciansky, P.-C., Hardenbol, J., Jacquin, T. and Vail, P.R., eds., 1998. Mesozoic and Cenozoic Sequence Stratigraphy of European Basins. *Spec. Publ. Soc. Sed. Geol.*, **60**.
- Dercourt, J., Ricou, L.E. and Vrielynck, B. (eds), 1993. *Atlas: Tethys Palaeoenvironmental Maps*. Gauthier-Villars, Paris.
- Dewey, J.F. and Pitman, W.C., 1998. Sea-level changes: mechanisms, magnitudes and rates. In: *Paleogeographic Evolution and Non-Glacial Eustasy, Northern South America* (J. L. Pindell and C. Drake, eds). *Spec. Publ. Soc. Sed. Geol.*, **58**, 1–16.
- Eyles, N., 1993. Earth's glacial record and its tectonic setting. *Earth-Sci. Rev.*, **35**, 1–248.
- Fairbridge, R.W., 1976. Convergence of evidence on climatic change and ice ages. *Ann. N. Y. Acad. Sci.*, **91**, 542–579.
- Frakes, L.A., Francis, J.E. and Syktus, J.I., 1992. *Climate Modes of the Phanerozoic*. Cambridge University Press, Cambridge.
- Gornitz, V., Lebedeff, S. and Hansen, J., 1982. Global sea-level trend in the past century. *Science*, **215**, 1611–1614.
- Gradstein, F.M., Agterberg, F.P., Ogg, J.G. *et al.*, 1995. A Triassic, Jurassic and Cretaceous time scale. In: *Geochronology, Time Scales and Global Stratigraphic Correlation* (W. A. Berggren *et al.*, eds). *Spec. Publ. Soc. Sed. Geol.*, **54**, 95–126.
- Gygi, R.A., 1995. Datierung von Seichtwassersedimenten des Späten Jura in der Nordwestschweiz mit Ammoniten. *Ecol. Geol. Helv.*, **88**, 1–58.
- Gygi, R.A. and Persoz, F., 1986. Mineralostratigraphy, litho- and biostratigraphy combined in correlation of the Oxfordian (Late Jurassic) formations of the Swiss Jura range. *Ecol. Geol. Helv.*, **79**, 385–454.
- Haq, B.U., Hardenbol, J. and Vail, P.R., 1987. Chronology of fluctuating sea levels since the Triassic. *Science*, **235**, 1156–1167.
- Hardenbol, J., Thierry, J., Farley, M.B. *et al.*, 1998. Charts. In: *Mesozoic and Cenozoic Sequence Stratigraphy of European Basins* (P.-C. De Graciansky *et al.*, eds). *Spec. Publ. Soc. Sed. Geol.*, **60**.
- Hillgärtner, H., 1998. Discontinuity surfaces on a shallow-marine carbonate platform (Berriasian, Valanginian, France and Switzerland). *J. Sediment. Res.*, **68**, 1093–1108.
- Hillgärtner, H., 1999. The evolution of the French Jura platform during the Late Berriasian to Early Valanginian: controlling factors and timing. *GeoFocus*, **1**, 203 pp.
- Hug, W.A., 2001. Sequenziell-dynamische Faziesentwicklung der karbonatisch-siliziklastischen Plattform im Oberen Oxford des Schweizer Jura. *GeoFocus*, **4**, in press.
- Jacobs, D.K. and Sahagian, D.L., 1993. Climate-induced fluctuations in sea level during non-glacial times. *Nature*, **361**, 710–712.
- Le Hegarat, G., 1971. Le Berriasien du Sud-Est de la France. *Doc. Lab. Géol. Fac. Sci. Lyon*, **43**.
- Lourens, L.J., Antonarakou, A., Hilgen, F.J. *et al.*, 1996. Evaluation of the Plio-Pleistocene astronomical timescale. *Paleoceanography*, **11**, 391–413.
- Lourens, L.J. and Hilgen, F.J., 1997. Long-period variations in the Earth's obliquity and their relation to third-order eustatic cycles and Late Neogene glaciations. *Quat. Int.*, **40**, 43–52.
- Miall, A.D., 1990. *Principles of Sedimentary Basin Analysis*, 2nd edn. Springer, Berlin.
- Miall, A.D., 1997. *The Geology of Stratigraphic Sequences*. Springer, Berlin.
- Mitchum, R.M. Jr, Vail, P.R. and Thompson, S. III, 1977. Seismic stratigraphy and global changes of sea level, part 2: The depositional sequence as a basic unit for stratigraphic analysis. In: *Seismic Stratigraphy – Applications to Hydrocarbon Exploration* (C. E. Payton, ed.). *Mem. Am. Ass. Petrol. Geol.*, **26**, 53–62.
- Montañez, I.P. and Osleger, D.A., 1993. Parasequence stacking patterns, third-order accommodation events, and sequence stratigraphy of Middle to Upper Cambrian platform carbonates, Bonanza King Formation, southern Great Basin. In: *Carbonate Sequence Stratigraphy* (R. G. Loucks and J. F. Sarg, eds). *Mem. Am. Ass. Petrol. Geol.*, **57**, 305–326.
- Pasquier, J.-B. and Strasser, A., 1997. Platform-to-basin correlation by high-resolution sequence stratigraphy and cyclostratigraphy (Berriasian, Switzerland and France). *Sedimentology*, **44**, 1071–1092.
- Pillans, B., Chappell, J. and Naish, T.R., 1998. A review of the Milankovitch climate beat: template for Plio-Pleistocene sea-level changes and sequence stratigraphy. *Sediment. Geol.*, **122**, 5–21.
- Pittet, B., 1996. Contrôles climatiques, eustatiques et tectoniques sur des systèmes mixtes carbonates-siliciclastiques de

- plate-forme: exemples de l'Oxfordien (Jura suisse, Normandie, Espagne). Unpubl. doctoral dissertation, University of Fribourg.
- Pittet, B. and Strasser, A., 1998a. Depositional sequences in deep-shelf environments formed through carbonate-mud import from the shallow platform (Late Oxfordian, German Swabian Alb and eastern Swiss Jura). *Eclog. Geol. Helv.*, **91**, 149–169.
- Pittet, B. and Strasser, A., 1998b. Long-distance correlations by sequence stratigraphy and cyclostratigraphy: examples and implications (Oxfordian from the Swiss Jura, Spain, and Normandy). *Geol. Rndsch.*, **86**, 852–874.
- Plint, A.G., Eyles, N., Eyles, C.H. and Walker, R.G., 1992. Control of sea level change. In: *Facies Models – Response to Sea Level Change* (R. G. Walker and N. P. James, eds), pp. 15–25. Geological Association of Canada, Alberta.
- Read, J.F., 1995. Overview of carbonate platform sequences, cycle stratigraphy and reservoirs in greenhouse and ice-house worlds. *Soc. Sed. Geol. Short Course*, **35**, 1–102.
- Schlager, W., Reijmer, J.J.G. and Droxler, A., 1994. Highstand shedding of carbonate platforms. *J. Sediment. Res.*, **B64**, 270–281.
- Schulz, M. and Schäfer-Neth, C., 1998. Translating Milankovitch climate forcing into eustatic fluctuations via thermal deep water expansion: a conceptual link. *Terra Nova*, **9**, 228–231.
- Schweigert, G., 1995. Amoebopeltoceras n.g., eine neue Ammonitengattung aus dem Oberjura (Ober-Oxfordium bis Unter-Kimmeridgium) von Südwestdeutschland und Spanien. *Stuttgart. Beitr. Naturk., Ser. B*, **227**, 1–12.
- Schweigert, G. and Callomon, J.H., 1997. Der bauhini-Faunenhorizont und seine Bedeutung für die Korrelation zwischen tethyalem und subborealem Oberjura. *Stuttgart. Beitr. Naturk., Ser. B*, **247**, 1–69.
- Shackleton, N.J., Hall, M.A., Raffi, I., Tauxe, L. and Zachos, J., 2000. Astronomical calibration age for the Oligocene–Miocene boundary. *Geology*, **20**, 447–450.
- Strasser, A., 1994. Milankovitch cyclicity and high-resolution sequence stratigraphy in lagoonal-peritidal carbonates (Upper Tithonian – Lower Berriasian, French Jura Mountains). In: *Orbital Forcing and Cyclic Sequences* (P. L. de Boer and D. G. Smith, eds). *Spec. Publ. Int. Ass. Sediment.*, **19**, 285–301.
- Strasser, A., Pittet, B., Hillgärtner, H. and Pasquier, J.-B., 1999. Depositional sequences in shallow carbonate-dominated sedimentary systems: concepts for a high-resolution analysis. *Sediment. Geol.*, **128**, 201–221.
- Strohmeier, C. and Strasser, A., 1993. Eustatic controls on the depositional evolution of Upper Tithonian and Berriasian deep-water carbonates (Vocontian Trough, SE France). *Bull. C.R. Expl.-Prod. Elf Aquitaine*, **17**, 183–203.
- Vail, P.R., Audemard, F., Bowman, S.A., Eisner, P.N. and Perez-Cruz, C., 1991. The stratigraphic signatures of tectonics, eustasy and sedimentology – an overview. In: *Cycles and Events in Stratigraphy* (G. Einsele et al., eds), pp. 617–659. Springer, Berlin.
- Vail, P.R., Mitchum, R.M. Jr and Thompson, S. III, 1977. Seismic stratigraphy and global changes of sea level, part 4: Global cycles of relative changes of sea level. In: *Seismic Stratigraphy – Applications to Hydrocarbon Exploration* (C. E. Payton, ed.). *Mem. Am. Ass. Petrol. Geol.*, **26**, 83–97.